ACS Catalysis

pubs.acs.org/acscatalysis
Research Article

Descriptors for Electrochemical CO_2 Reduction in Imidazolium-Based Electrolytes

Federico Dattila, Alessia Fortunati, Federica Zammillo, Hilmar Guzmán, Núria López,* and Simelys Hernández*

Cite This: ACS Catal. 2024, 14, 16166−16174
Read Online

ACCESS | Metrics & More | Article Recommendations | Supporting Information

ABSTRACT: Electrochemical CO_2 reduction (CO_2R) allows us to close the carbon cycle and store intermittent renewable energy into chemical products. Among these, syngas, a mixture of hydrogen and carbon monoxide, is particularly valuable due to its high market share and the low energy required for its electrocatalytic production. In addition to catalyst optimization, lately, electrolyte modifications to achieve a suitable CO/H_2 ratio have also been considered. Ionic liquid (IL)-based electrolytes have enabled high faradaic efficiency toward CO, depending on the chemical properties of the IL. In this work, we rationalized through density functional theory (DFT) descriptors the competition between hydrogen evolution (HER) and CO_2R on silver in imidazolium-based electrolytes, developing a DFT-based analytical model. The electrolyte anion regulates the concentration ratio between cationic and carbene species of ILs cation, respectively, between the 1-ethyl-3-methylimidazolium cation ($EMIM^+$) and carbene (EMIM:) species and between the 1-butyl-3-methylimidazolium cation ($BMIM^+$) and carbene (BMIM:). The latter species, if formed, hinders the CO_2R by blocking the active sites or trapping CO_2 in solution. In the case of weak Lewis base anions as fluorinated ones, $EMIM^+$ ($BMIM^+$) cations, which serve as cocatalysts in CO_2R, are more abundant, allowing high CO partial current densities and high electrochemically active surface area. Applying the here-defined descriptors to ILs not yet tested makes it possible to predict the HER and CO_2R selectivity on silver, thus enabling guidelines for designing better ILs for CO_2R.

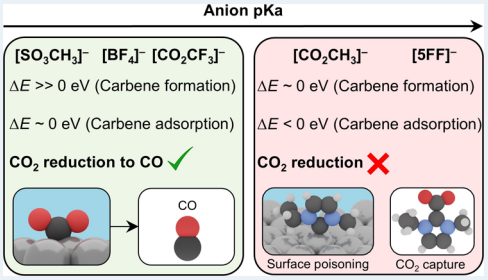

KEYWORDS: *electrochemical CO_2 reduction, ionic liquids, anion effect, syngas, surface poisoning*

INTRODUCTION

The electrochemical reduction of carbon dioxide (CO_2R) is a promising technology for reducing CO_2 atmospheric concentration by simultaneously storing renewable energy and generating high-value-added products.[1] Among the many possible reaction products, the generation of syngas, *i.e.*, the mixture of carbon monoxide (CO) and hydrogen (H_2), is particularly appealing as it requires low energetic consumption (being a 2-electrons reaction) when compared to other reduction products, yet it ensures a broad market share.[2−4] Since the reports by Hori and co-workers,[5] such a process usually occurs on weak CO-binding catalysts, like Au and Ag.[6] Several strategies to modify the microenvironments close to the electrode have been put forward.[7] Among these approaches, ionic liquids (ILs) can have a beneficial effect on the process.[8,9] At room temperature (298.15 K) and standard pressure (1 atm), CO_2 and CO concentrations in ionic liquid electrolytes account for ∼0.02 mol % and ∼2−3 mM, respectively.[10,11] Thus, they are generally significantly higher than the aqueous limit, i.e., 6×10^{-4} and 1.8×10^{-5} mol % (33 and 1 mM considering water molarity, 55 M),[12,13] due to better solubility.

Earlier mechanistic and computational studies offered divergent explanations for the role of IL. ILs can either stabilize via electrostatic interaction the CO_2 adsorbate[14,15] similar to metal cations in aqueous electrolytes,[16] poison the surface,[17] thus blocking CO_2 reduction and enhancing the hydrogen evolution reaction (HER) via water reduction, or affect water and CO_2 diffusion to the surface.[18] Neyrizi et al.[19] recently summarized the three potential effects of imidazolium cations (a common constituent of ILs): (i) suppress HER by hindering H_3O^+ migration (as observed in acidic media);[20] (ii) favor the formation of an imidazolium carboxylate intermediate along the CO_2 reduction route;[21−23] and/or (iii) stabilize the $*CO_2$ intermediate via short-term electrostatic interactions.[14] Besides, the authors introduced another promotional effect in anhydrous electrolyte, *i.e.*, the promotion of the proton-coupled electron transfer from C_2-H to chemisorbed CO_2.[19]

Received: August 20, 2024
Accepted: September 30, 2024
Published: October 17, 2024

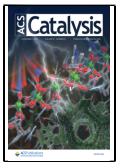

Urushihara et al.,[17] instead, highlighted potential poisoning effects on silver due to 1-ethyl-3-methylimidazolium cation ($EMIM^+$) adsorption (coverages larger than 1/9 monolayer for potentials more negative than −0.5 V vs SHE). Sharifi Golru et al. first highlighted the relevance of IL anions. Their preliminary report suggested that more hydrophilic anions, such as dicyanamide (DAC), determine a higher water concentration at the cathode and a lower CO_2 affinity, thus boosting HER.[18] Instead, hydrophobic anions enable a high CO_2 availability at the surface, promoting the generation of CO_2R products (formate, in their experiment).[18] In a later study, they confirmed this hypothesis via a multiphysics model, showing low CO_2 concentration and high surface pH for hydrophilic anions such as DAC.[24]

In search of simple descriptors of the IL performance, Neyrizi et al. deemed C_2H acidity responsible for enhanced hydrogen evolution in imidazolium-based media.[19] Regarding the CO_2R performance, we recently carried out an experimental screening of the CO_2R performance of seven different 1-ethyl-3-methylimidazolium ($EMIM^+$)/1-butyl-3-methylimidazolium ($BMIM^+$)-based ionic liquids on silver electrodes. In such joint experimental/theoretical work,[15] some of us hypothesized that the Lewis basicity of IL anions tunes the equilibrium between the cations ($EMIM^+$ or $BMIM^+$) and their neutral corresponding carbenes (EMIM: and BMIM:). If formed, these carbenes poison the surface or capture CO_2, promoting HER, while imidazolium cations act as CO_2R cocatalysts. Although we proved the existence of adsorbed carbenes via Raman spectroscopy and demonstrated the cocatalyst role of $EMIM^+$ or $BMIM^+$ via density functional theory (DFT) simulations, the role of anions remained qualitative.

In this work, we investigate the role of IL with different anions and cations via DFT simulations and experiments to rationalize and expand the previous knowledge. We unravel three simple thermodynamic descriptors, justifying the selectivity trends observed experimentally in imidazolium-based electrolytes. Based on these DFT descriptors, we develop an analytical model to correlate surface concentrations of IL species to CO selectivity. By extending the framework introduced here to novel ILs, their performance for HER and CO_2R on silver could be predicted before experimental assessment, thus preventing time-consuming laboratory screenings.

RESULTS AND DISCUSSION

Experimental Results. Chronopotentiometry measurements were carried out for t = 2 h on silver foil at j_{tot} = −20 mA cm^{-2} applied current density in seven specific imidazolium-based ionic liquids in acetonitrile, ACN (see Experimental Methods in the Supporting Information; further details are available in ref 15). The use of this electrolyte (imidazolium-based ionic liquids in ACN) enables high CO_2 solubility, thus allowing high CO_2 surface concentration, which is beneficial for CO production. CO_2 solubility in ACN (the main component of the electrolyte) is reported up to 240 mM, while the CO_2 solubility is 33 mM in aqueous media.[12] The CO_2 reduction was favored in the presence of fluorinated-based anions (*i.e.*, weak Lewis bases), and consequently, high constant CO production was observed, see Figure 1. We attribute such an effect to the stabilization of CO_2 by $BMIM^+$, as proposed in refs 14,15. Instead, by employing acetate $[CO_2CH_3]^-$ anions (*i.e.*, strong Lewis bases), the conversion of

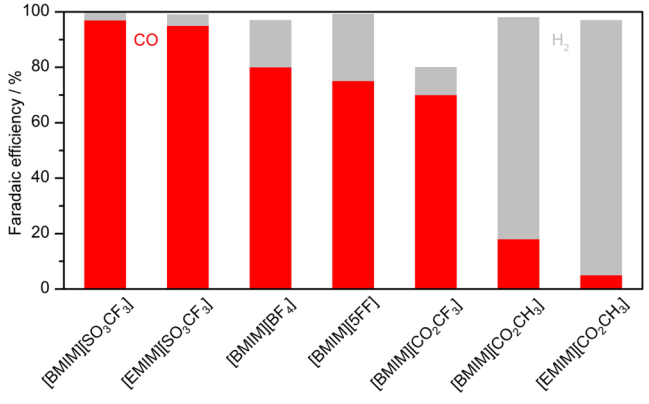

Figure 1. Experimental results for CO_2 reduction at j_{tot} = −20 mA cm^{-2} on a silver foil in imidazolium-based ionic liquids. Faradaic efficiency toward CO is reported in red, while H_2 selectivity is indicated in gray. The experimental setup consisted of an H-cell, Ag foil as a working electrode, Ni mesh as a counter electrode, 0.3 M IL in ACN as catholyte, and 0.1 M KOH as the anolyte.

CO_2 was hindered. We linked such a change to the evolution of $BMIM^+$ to BMIM:. Carbenes are expected to poison the surface or capture CO_2, increasing H_2 production. The electrochemical tests resulted in a singular selectivity switch between CO-selective (with triflate $[SO_3CF_3]^-$ as anions) and H_2-selective electrolytes (with acetate as anions), independently of the applied current densities.[15] The roles of $EMIM^+$ and $BMIM^+$ cations in the selectivity seemed instead to be marginal. Remarkably, a linear correlation exists between anion's pK_a (calculated in aqueous media) and the CO/H_2 selectivity ratio for $BMIM^+$-based electrolytes (see Supporting Figure 1). Such a CO/H_2 selectivity ratio trend is confirmed for different values of applied current densities (see Supporting Figure 2).

Reaction Mechanisms in Imidazolium-Based CO_2 Saturated Electrolytes. According to the state-of-the-art,[25−27] summarized in the recent work by Fortunati et al.,[15] few relevant reactions occur in imidazolium-based CO_2-saturated electrolytes. First, equilibrium reactions take place in the bulk electrolyte. Particularly, given the Lewis basicity of the anions, the proton (H^+) exchange equilibrium between $EMIM^+$-anion can favor the evolution of these cations to carbenes (Figure 2a, see Supporting Figure 3a for $BMIM^+$). Acetate being a strong Lewis base (high pK_a in aqueous media), this reaction is shifted toward the formation of carbenes; i.e., lower energy is required to form carbenes, ΔE_{form} (EMIM:), see Figure 2a(1). The reaction to form BMIM: is reported in Supporting Figure 3a(1). Thus, a significant amount of carbene forms in acetate-based IL electrolytes. If we instead consider weak Lewis bases (low pK_a in aqueous media), such as $[CO_2CF_3]^-$, for instance, its basic strength to tear the C_2−H from $EMIM^+$ is reduced; thus the formation of carbene is hindered, *i.e.*, higher energy of formation is required, ΔE_{form} (EMIM:) ≫ 0. Such is the case also for fluorinated anions, such as $[SO_3CF_3]^-$ and $[BF_4]^-$, see Figure 2a(2). The analogous reaction scheme for BMIM is reported in Supporting Figure 3a(3).

If carbenes form, they can either react with dissolved CO_2 in solution to form carboxylates or adsorb on the Ag catalyst surface (Figures 2b, Supporting Figure 3b). Chiarotto et al.[28] experimentally observed the presence of carbenes in acetate-based ILs and their subsequent reaction with CO_2 to form

https://doi.org/10.1021/acscatal.4c05012
ACS Catal. 2024, 14, 16166−16174

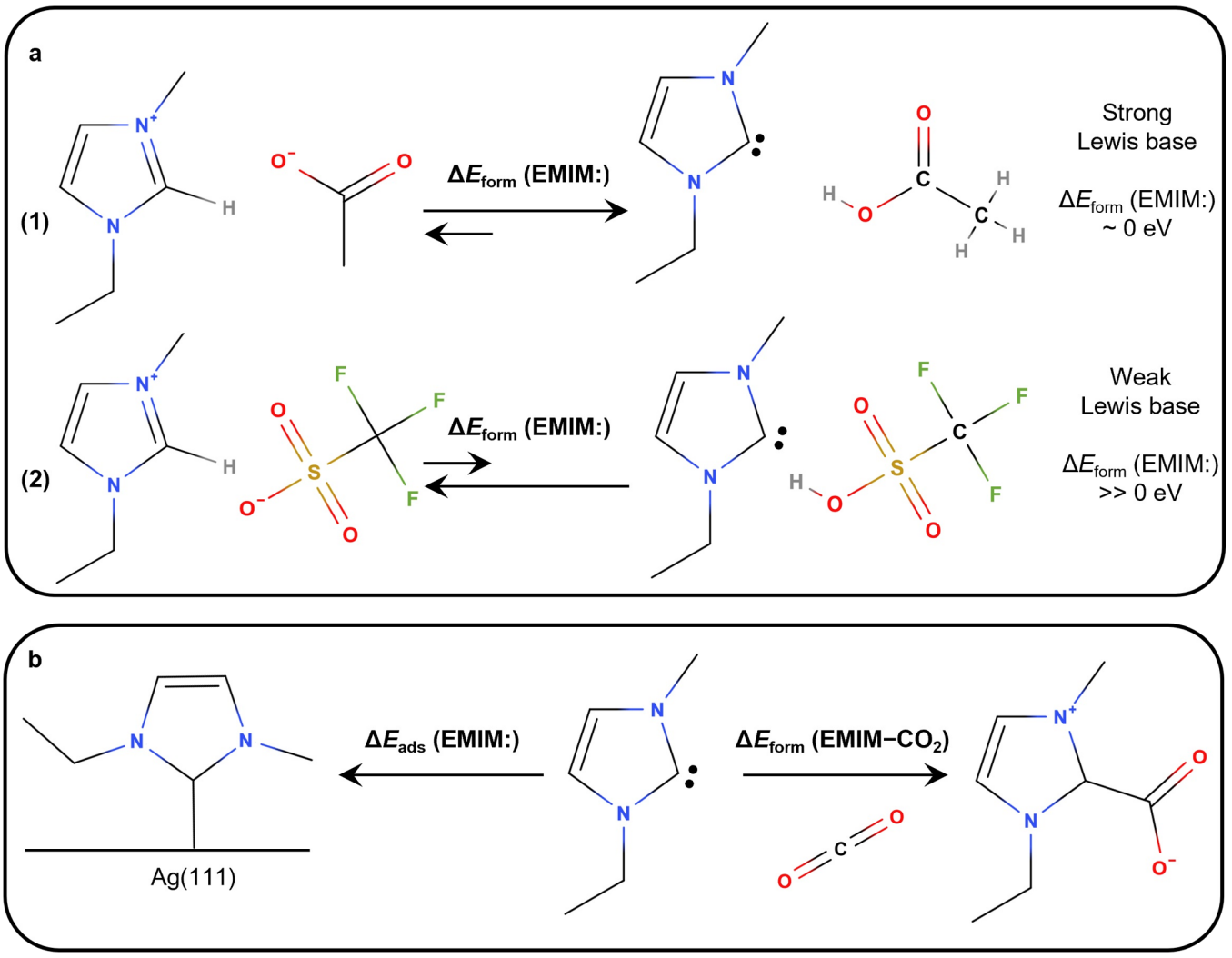

Figure 2. (a) Formation of carbenes from the homogeneous reaction between $EMIM^+$ and the anion species. The formation energy of the carbene, ΔE_{form} (EMIM:), depends on anion basicity. (b) Reactions of carbenes with Ag(111) and CO_2. Once formed, carbenes can either adsorb on the catalytic surface, thus poisoning it, or capture CO_2 from the solution, thus forming a carboxylate complex. The reaction scheme for interaction between $BMIM^+$ and anion species and $BMIM^+$/BMIM: equilibrium is reported in Supporting Figure 3.

BMIM–CO_2 carboxylates. Such a process was confirmed by the evolution of acetate to acetic acid after the release of C_2 hydrogen release from the ring. Besides, the formation of carboxylate has been heavily investigated via DFT,[26,27] and the use of acetate-based ionic liquids as CO_2 sorbent is well known in the field.[29] The poisoning effect of imidazolium cations on Ag has already been observed, and coverages higher than 1/9 ML have been proposed for the applied potential that is more negative than −0.5 V vs SHE via a DFT study.[17] If carbenes do not form, as in the case of weak Lewis base anions, then the interaction of IL cations with CO_2 and the catalyst surface is negligible and mainly occurs via weak van der Waals forces.

Dependence of H_2 Selectivity vs Carbene Formation. Given the previous considerations, we moved to DFT simulations to identify descriptors and rationalize the role of IL anions. We modeled the experimental system (polycrystalline silver foil) with a four-layer-thick Ag(111) p(3 × 3) supercell (see Figure 3). Then, one ionic liquid unit was inserted in solution, including as cation $EMIM^+$ (or $BMIM^+$) and as anion one among acetate, trifluoroacetate, triflate, tetrafluoroborate, and pentafluorophenol (see Figure 3). The effect of the seven resulting cation–anion pairs on CO_2R was assessed through the PBE density functional,[30] corrected for dispersion via the DFT-D2 method. Further computational details are available in the Supporting Information. Since the presence of carbenes seems instrumental in the selectivity switch between H_2 and CO,[15] we tentatively assessed the dependence of the experimental partial current density toward H_2 (for j_{tot} = −20 mA cm^{-2}, see Figure 4) with respect to the energy required to form a carbene from an $EMIM^+$/$BMIM^+$ cation, i.e., ΔE_{form} (EMIM:/BMIM:). In fact, the low formation energy characteristic of acetate anions corresponds to higher H_2 evolution activities, while anions that hardly promote carbenes formation, such as $[SO_3CF_3]^-$, minimize H_2 production. The qualitative trend between partial H_2 current density and carbene formation energies resembles a Langmuir isotherm,[31] suggesting a coverage phenomenon that reaches saturation for acetate anions. Such Langmuir dependence is also observed by analyzing the H_2 partial current density versus anion's pK_a for $BMIM^+$-based electrolytes (see Supporting Figure 4).

As a final note on H^+ sources, given the water content of acetate-based ionic liquids (0.7%) and their volume in the catholyte (2.3 and 1.8 mL, respectively for $[BMIM][CO_2CH_3]$

https://doi.org/10.1021/acscatal.4c05012
ACS Catal. 2024, 14, 16166−16174

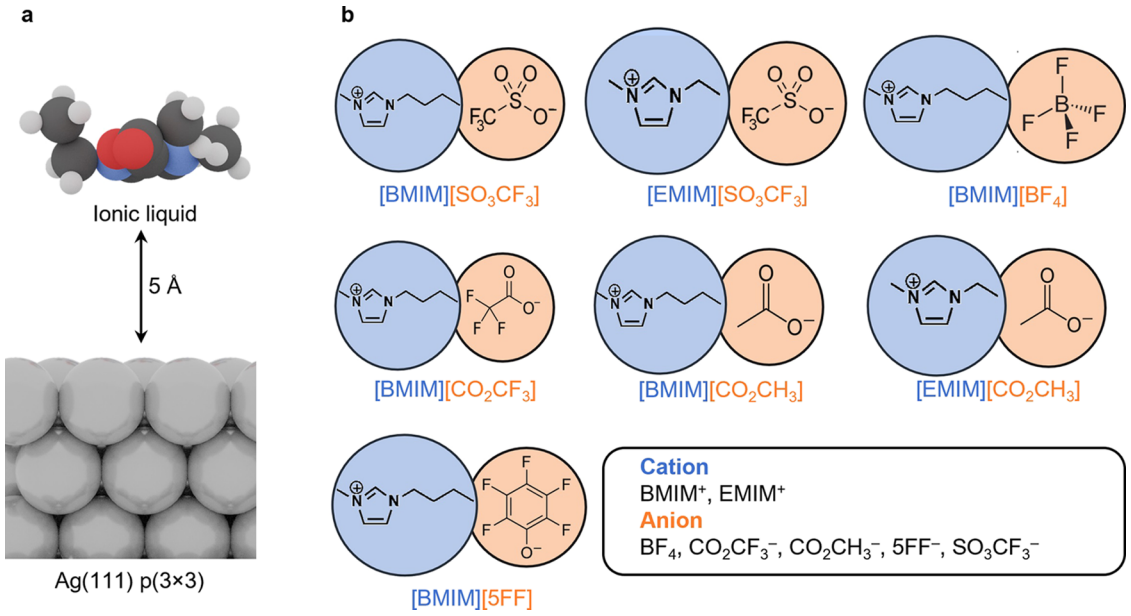

Figure 3. (a) Side view of the DFT model employed. Ionic liquids were placed in the vicinity of an Ag(111) p(3 × 3) supercell. (b) Summary of the imidazolium-based ILs tested in ACN as electrolytes for CO_2R. Blue boxes indicate cations, while orange species are the corresponding anions.

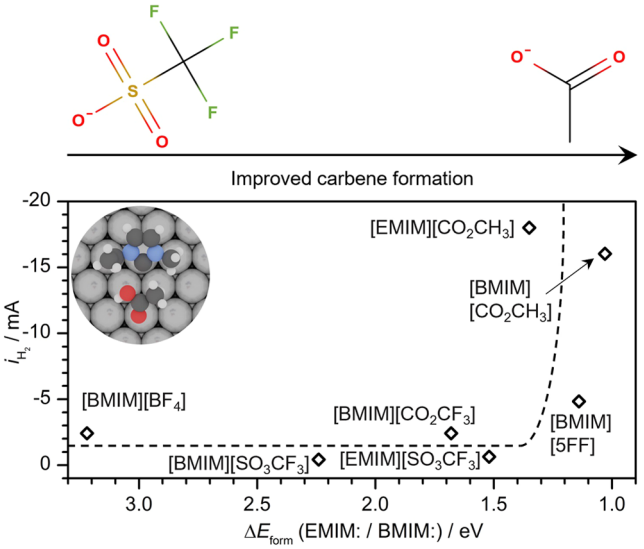

Figure 4. Dependence of the partial current toward H_2 on the formation energy of carbenes (EMIM:/BMIM:). The dashed line serves as a guide for the eye and reproduces a Langmuir isotherm. The total applied current density was $j_{tot} = -20$ mA cm^{-2}.

and [EMIM][CO_2CH_3], see Tables S1 and S2), the maximum expected water volume should be around 16.1 and 12.1 μL, respectively. Besides, lower energy to form carbenes naturally implies a more favorable release of the C_2-H from the imidazolium ring, so consequently, a higher concentration of H^+ is available for reduction. This may also explain the increase in H_2 selectivity for low values of ΔE_{form} (EMIM:/BMIM:) (Figure 4). Nevertheless, our previous work considered the main H^+ source as those generated by the bipolar membrane or water from anolyte crossover rather than from [BMIM]/[EMIM] protons or H_2O impurities.[15] In fact, at the experimental conditions employed (t = 2 h of CO_2R at j_{tot} = −20 mA/cm^2, see Figure 1), such a water volume would only imply a difference in H_2 faradaic efficiency of around 20% (see Supporting Figure 5), not enough to explain the drastic change between acetate-based electrolytes and the other ILs (at least 45%, see Figure 1).

Dependence of CO Selectivity vs Carbene Formation. Moving to the electrochemical reduction of CO_2, we can shortlist the interactions between carbenes and CO_2 to mainly two detrimental effects. Once these species form, they can (i) capture CO_2 or (ii) adsorb on the electrode surface. Thus, we tentatively defined the adsorption energy of carbenes, *i.e.*, ΔE_{ads} (EMIM:/BMIM:), and the formation of carbene-CO_2 complexes, *i.e.*, carboxylates, ΔE_{form} (EMIM−CO_2/BMIM−CO_2) as descriptors to rationalize the CO selectivity on the seven considered imidazolium-based electrolytes (Figure 5). Indeed, a peak of the CO partial current density is observed for the [SO_3CF_3] anions, implying low values of carbene adsorption and carboxylate formation energies. Instead, for

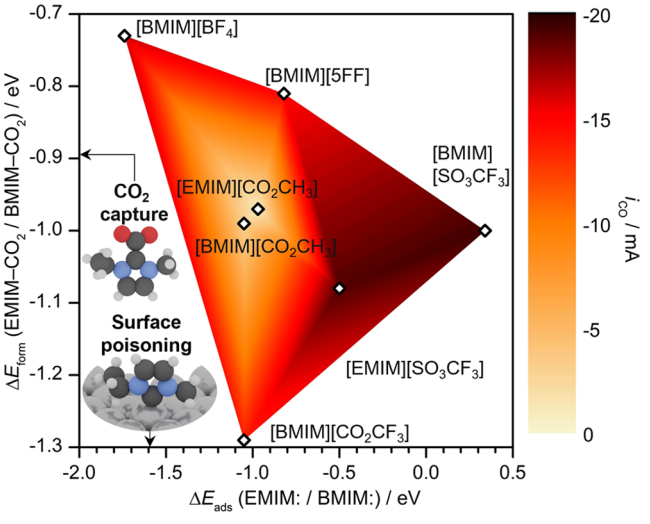

Figure 5. Dependence of partial current toward CO on adsorption energy of carbenes (EMIM:/BMIM:, x-axis) and formation energy of carboxylates (EMIM/BMIM-CO_2, y-axis). The total applied current density was $j_{tot} = -20$ mA cm^{-2}.

https://doi.org/10.1021/acscatal.4c05012
ACS Catal. 2024, 14, 16166−16174

stronger binding of carbenes to the surface as for the acetate anions, reduction of the amount of CO_2 to CO is hindered, further confirming a surface poisoning effect. Besides, a Langmuir dependence is found between CO partial current densities and anion's pK_a for $BMIM^+$-based electrolytes (see Supporting Figure 6), with an opposite trend than HER dependence (Supporting Information, Figure 4). Remarkably, the CO selectivity is higher for the $[CO_2CF_3]$ anion than for acetate, although the former is characterized by a more exothermic formation of carboxylates. We highlight here that carbenes' adsorption and formation of carboxylates are competing processes since, once a carboxylate forms, the carbene precursor cannot poison the surface anymore. Thus, for the $[CO_2CF_3]$ anion, a more favorable formation of carboxylates involves a lower concentration of free carbenes in solution able to poison the surface, thus a partial positive effect of the electrochemical CO_2 reduction reaction compared to the acetate anion.

Experimental Validation. In the previous sections, we showed via DFT that carbene formation crucially affects the CO_2R selectivity between HER and CO for imidazolium-based electrolytes. If formed, carbenes poison the surface or capture CO_2 in solution, thus hindering the CO_2R and leading to an increase in HER. To prove our hypothesis, we sought further experimental validation.

Electrochemically active surface area (ECSA) values were determined for the Ag foil in the presence of $EMIM^+$ ($BMIM^+$) acetate and triflate (0.3 M in ACN) in a CO_2- and N_2- saturated environment (see Experimental Details and Supporting Table 3 for additional details). The use of ECSA to assess surface poisoning effects is common in the field; for instance, Ohyama et al. reported the dependence on electrolyte pH of ECSA values for Pt/C catalysts due to OH^- poisoning during hydrogen oxidation reaction.[32] Although the same catalyst was used for the test in both CO_2- and N_2-saturated electrolytes, the ECSA is higher for the $[SO_3CF_3]^-$ anion than the $[CO_2CH_3]^-$ one. Remarkably, ECSA values show a Langmuir dependence on carbene formation energy (Figure 6a) and carbene adsorption energy (Figure 6b). Specifically, weak Lewis anions such as triflate show no interaction with the surface, thus constant ECSA values. At the same time, the active area decreases in the presence of acetate, suggesting a poisoning effect.

The correct use of carbene formation energy as the principal descriptor for CO/H_2 competition was further confirmed by a selected experiment with a methylated-BMIM complex in the presence of acetate anion, still in ACN. While the original complex shows poor CO selectivity at j_{tot} = −20 mA cm^{-2} (<20%), the methylated-BMIM cation determines an increase of CO faradaic efficiency up to more than 60% (Figure 6c). Such a change was attributed to a less favorable release of C_3 and C_4 hydrogens from the BMIM ring and a consequent higher formation energy for carbene (see Supporting Figure 7 for the process scheme). According to DFT, such a process is in fact 0.3 eV more endothermic than the release of C_2-H on $[BMIM][CO_2CH_3]$.

As a final validation, we experimentally assessed the CO_2 reduction performance of the Ag foil in the presence of a mixed BMIM acetate/triflate electrolyte in 3-methoxypropionitrile (3-MPN). This experiment was carried out in 3-MPN rather than ACN to extend the experimental study to a similar solvent with a higher boiling point (thus able to support the application at higher temperatures). In this way, we could also rule out any potential effect on the H_2/CO selectivity by the solvent. Details on methods and the molar concentrations of the ionic liquids are reported in the Supporting Information (see corresponding section and Supporting Information Table 4). In line with our hypothesis, an increase in acetate/triflate molar ratio led to an improved H_2 selectivity vs CO (Figure 6d). Again, such dependence resembles a Langmuir isotherm, thus suggesting that an increase in acetate concentration determines a higher concentration of carbenes, which hinders the reduction of CO_2 by poisoning the surface or capturing CO_2 in solution.

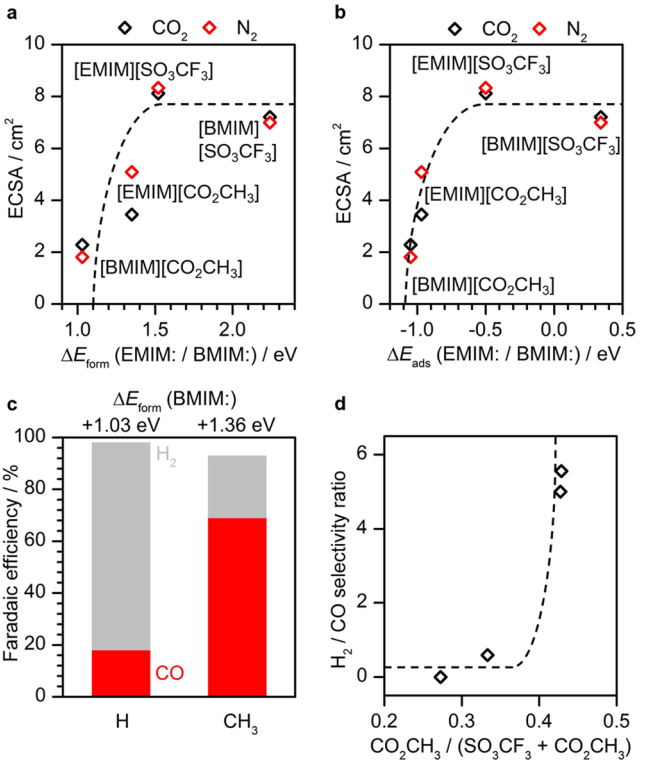

Figure 6. Dependence of the ECSA on (a) the formation energies of carbenes and (b) the adsorption energies of carbenes for both CO_2-saturated (black points) and N_2-saturated (red points) electrolytes. In both cases, the dashed lines guide the eye and reproduce a Langmuir isotherm. (c) Improvement of CO selectivity of polycrystalline Ag in the methylated-$[BMIM][CO_2CH_3]$ vs $[BMIM][CO_2CH_3]$ in ACN at a total applied current density of j_{tot} =−20 mA cm^{-2}. The top values are the formation energies of BMIM: carbenes for both cases. (d) Langmuir dependence between the H_2/CO selectivity ratio at j_{tot} = −20 mA cm^{-2} and the molar ratio between acetate and triflate in $[BMIM][CO_2CH_3]/[SO_3CF_3]$ in 3-methoxypropionitrile.

Analytical Model. Based on our insights, carbene formation energy and carbene adsorption are the main components responsible for the selectivity switch between H_2 and CO in such experimental systems. Taking inspiration from an analogous report for alkali cations in an aqueous environment,[33] it is then possible to derive an analytical framework for the overall process. For the sake of simplicity, we limited the discussion to the $[BMIM][CO_2CH_3]$ electrolyte. However, it can be generalized to other IL pairs.

As defined in Figure 2a, the homogeneous reaction between the cation and anion follows eq 1. Thus, the concentration of carbenes depends on the bulk concentration of BMIM cations and the forward rate constant of carbene formation (k_{form}), see eq 2.[31] To include adsorption processes, we can now recall the

https://doi.org/10.1021/acscatal.4c05012
ACS Catal. 2024, 14, 16166−16174

definition of the Langmuir isotherm,[31] which relates the surface coverage of a certain species (θ, given in monolayer) to the rate constant for adsorption (k_{ads}) and the bulk concentration of the adsorbate precursor (in this case, BMIM:, see eq 3). By recalling eq 2, we can define a univocal analytical equation linking the BMIM: surface coverage to the bulk $BMIM^+$ concentration, as shown in eq 4.

Both carbene formation and carbene adsorption rate constants can be expressed in terms of the relative DFT energies under the assumption of linear scaling relationships between ΔE and activation energies, ref[31,34] see eqs 5 and 6, thus confirming analytically that favorable formation and then adsorption of carbenes (very high k_{form}, k_{ads}) lead to high BMIM: surface coverages (very high θ) and consequently inhibition of CO_2 reduction (see Supporting Figure 8).

$$BMIM^+ + CH_3COO^- \xrightarrow{\Delta E_{form}(BMIM:)} BMIM: + CH_3COOH \quad (1)$$

$$[BMIM:] \sim k_{form}[BMIM^+] \quad (2)$$

$$\frac{\theta}{1-\theta} \sim k_{ads}[BMIM:] \quad (3)$$

$$\theta = \frac{1}{1 + \frac{1}{k_{form} * k_{ads}[BMIM^+]}} \quad (4)$$

$$k_{form} \sim \exp\left(-\frac{\Delta E_{form}(BMIM:)}{k_B T}\right) \quad (5)$$

$$k_{ads} \sim \exp\left(-\frac{\Delta E_{ads}(BMIM:)}{k_B T}\right) \quad (6)$$

The correctness of the developed analytical model is confirmed by the strong correlation between the faradaic efficiency toward CO observed experimentally for the five BMIM-based electrolytes at $j_{tot} = -20$ mA/cm^2 and the simulated availability of Ag active sites, calculated through eq 4 for 1 M $BMIM^+$ concentration, $k_{ads} = 10$, and $k_{form} = 0-7$, see Figure 7. EMIM-based electrolytes are omitted from the analysis, as our experimental data set is limited to two data points. Electrolytes characterized by weak Lewis base anions (e.g., $[BF_4]^-$, $[SO_3CF_3]^-$) present very endothermic carbene formation energies, so those formation rates are negligible. Consequently, for these species, the availability of Ag sites is maximized, and CO selectivity reaches its maximum. Instead, ILs with strong Lewis bases, such as $[CO_2CH_3]^-$, show low carbene formation energies, thus achieving high formation rates. Once formed, carbene poisons the surface, leading to a sharp decrease in the number of active sites available; see the dashed line in Figure 7.

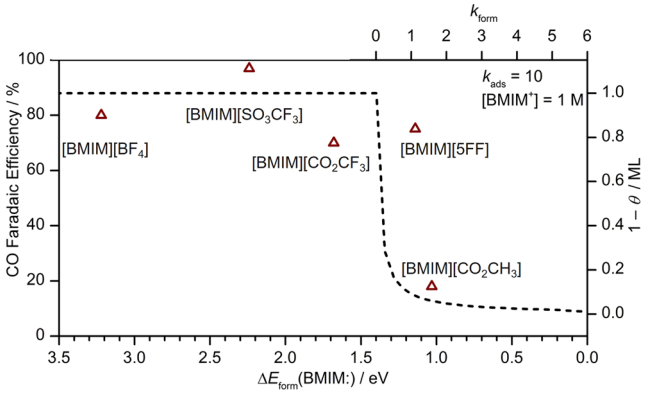

Figure 7. Correlation between experimental faradaic efficiencies toward CO (right y-axis) for the five BMIM-based electrolytes tested at $j_{tot} = -20$ mA/cm^2 of applied current densities and BMIM: formation energy (bottom x-axis). The dashed line indicates the simulated availability of active sites ($1 - \theta$, left y-axis) vs the rate of BMIM: formation (top x-axis).

Selectivity Map. Overall, we can then identify two main selectivity regions for the seven imidazolium-based electrolytes considered (Figure 8) by correlating the experimental partial CO and H_2 currents at $j_{tot} = -20$ mA/cm^2 with the DFT formation energy of EMIM:/BMIM: carbenes and their DFT adsorption energy. According to reaction mechanisms reported in Figure 2a(2), fluorinated anions are characterized by high carbene formation energy, *i.e.*, low formation rate, k_{form}. This leads to low values of carbene surface coverage. Consequently, the reduction of CO_2 to CO occurs. On the other side, as shown in Figure 2a(1), acetate shows a lower carbene formation energy, *i.e.*, a high rate constant of formation, k_{form}, and a mild to strong adsorption energy, *i.e.*, a high rate constant of adsorption, k_{ads}. In line with eq 7 and Supporting Figure 8, in this case, carbenes effectively poison the surface, thus hindering CO production and limiting the electrocatalytic reactions to HER.

Outlook. The joint experimental and computation insights here reported let us determine the relative importance of each of the players involved in the process. Although this study is limited to silver, it can be generalized to other heterogeneous catalysts. In fact, any significant influence of the catalyst on the process lies within the interaction with the imidazolium carbene, *i.e.*, the ΔE_{ads} (EMIM:/BMIM:) descriptors and its reactivity with the CO_2R intermediates. Thus, a catalyst different from Ag may show a CO_2R product distribution beyond CO and a different extent of surface poisoning. For instance, stronger binding elements such as Cu exhibit more negative ΔE_{ads} (EMIM:/BMIM:), see Supporting Figure 9, and thus are expected to be more affected by surface poisoning. In particular, a linear scaling relationship between ΔE_{ads} (EMIM:/BMIM:) and the metal d-band center occurs, in line with the well-known d-band model.[35−37] Instead, the nature of the imidazolium itself, either the 1-ethyl-3-methylimidazolium or 1-butyl-3-methylimidazolium cation, does not show any influence in the process. The choice of the anion is crucial to determine the selectivity between the CO_2R products (here CO) and H_2.

Once the appropriate catalyst is chosen, weak Lewis base anions should be considered to maximize the level of CO_2R in organic solvents. In contrast, strong Lewis base ones may be employed to promote HER via surface poisoning. Finally, appropriate tuning of IL concentration in organic solvents, as well as mixing with inorganic cations, may allow for the prevention of surface poisoning effects and the parallel CO_2 capture and conversion processes through acetate-based electrolytes.

CONCLUSIONS

In this work, we have defined a general DFT-based analytical framework to rationalize the role of anions in imidazolium-based electrolytes for electrochemical CO_2 reduction. Based on experimental observations on seven IL pairs, we have identified carbene formation energy and carbene adsorption energy as

https://doi.org/10.1021/acscatal.4c05012
ACS Catal. 2024, 14, 16166−16174

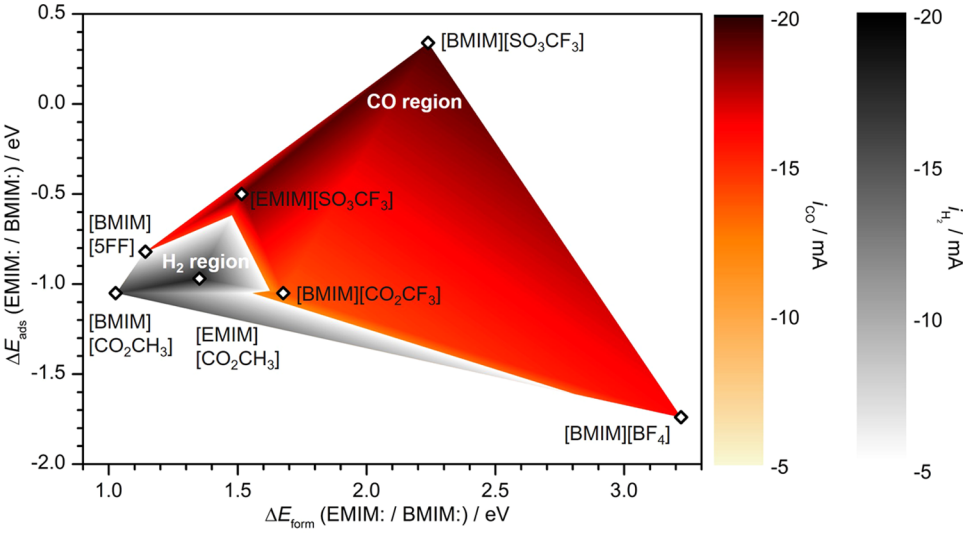

Figure 8. Formation energy of EMIM:/BMIM: carbenes (*x*-axis) and their adsorption energy (*y*-axis) as descriptors of H_2 (gray area) and CO (red area) selectivity for different imidazolium-based ILs on the Ag foil. The intensity of gray and red depends on the experimental partial current density for H_2 and CO, respectively, taken from Figure 1 (see the color scale on the right columns).

the two crucial descriptors that rule the competition between H_2 and CO production during CO_2R. Specifically, in the presence of strong Lewis base anions, carbenes form from imidazolium cations and either block the active sites or capture CO_2 in solution, thus preventing CO_2 reduction. Weak Lewis base anions make carbene formation and adsorption on the surface highly endothermic, thus preventing surface poisoning and enabling CO generation. Starting from the two proposed descriptors, the CO_2 reduction performance of future imidazolium-based electrolytes could be predicted, guiding the rational design of the IL and the selection of the most promising ones to promote selectivity toward the desired products.

■ ASSOCIATED CONTENT

Supporting Information

The Supporting Information is available free of charge at https://pubs.acs.org/doi/10.1021/acscatal.4c05012.

Experimental and computational methods; additional correlations between experimental partial current densities and descriptors; additional details on the electrochemical surface area measurements and the electrochemical CO_2 reduction tests on IL mixtures; the reaction scheme for carbene formation from C_3 and C_4H; simulated carbene coverages vs bulk imidazolium concentration (PDF)

The data sets generated through DFT and analyzed during the current study are available in the ioChem-BD database[38] at DOI: 10.19061/iochem-bd-1-306[39]

■ AUTHOR INFORMATION

Corresponding Authors

Núria López − *Institute of Chemical Research of Catalonia (ICIQ-CERCA), The Barcelona Institute of Science and Technology (BIST), 43007 Tarragona, Spain;* orcid.org/0000-0001-9150-5941; Email: nlopez@iciq.es

Simelys Hernández − *CREST Group, Department of Applied Science and Technology (DISAT), Politecnico di Torino, 10129 Turin, Italy;* orcid.org/0000-0002-6722-0273; Email: simelys.hernandez@polito.it

Authors

Federico Dattila − *CREST Group, Department of Applied Science and Technology (DISAT), Politecnico di Torino, 10129 Turin, Italy;* orcid.org/0000-0001-8195-3951

Alessia Fortunati − *CREST Group, Department of Applied Science and Technology (DISAT), Politecnico di Torino, 10129 Turin, Italy;* Present Address: Present Address: Istituto Italiano di Tecnologia, Via Livorno 60, 10144 Torino, Italy

Federica Zammillo − *CREST Group, Department of Applied Science and Technology (DISAT), Politecnico di Torino, 10129 Turin, Italy*

Hilmar Guzmán − *CREST Group, Department of Applied Science and Technology (DISAT), Politecnico di Torino, 10129 Turin, Italy;* orcid.org/0000-0002-0536-2233

Complete contact information is available at: https://pubs.acs.org/10.1021/acscatal.4c05012

Author Contributions

F.D., A.F., and F.Z. wrote the manuscript, with input from all authors. S.H. designed the experiments. A.F. carried out the CO_2 electroreduction experiments with single and mixed ionic liquids. F.D. designed and carried out the DFT simulations in collaboration with N.L. F.Z. and H.G. carried out the ECSA measurements. All authors read and commented on the manuscript and approved the final version.

Funding

SUNCOCHEM-862192 by European Commission. SEVERO OCHOA GRANT by the Spanish Ministry of Science and Innovation.

Notes

The authors declare no competing financial interest.

■ ACKNOWLEDGMENTS

This work was supported by the European Commission through the European Union's Horizon 2020 Research and Innovation Action program under the SunCoChem project

(Grant Agreement No. 862192). F.D. and N.L. further acknowledge the financial support by the Spanish Ministry of Science and Innovation (PID2021-122516OI00, Severo Ochoa Grant MCIN/AEI/10.13039/501100011033CEX2019-000925-S) and the Barcelona Supercomputing Center (BSC-RES) for providing generous computational resources. F.D. and S.H. acknowledge the CINECA award under the ISCRA initiative for the availability of high-performance computing resources and support within the ILCO$_2$SYN project. F.Z. thanks Fondazione CRT for the financial support.

REFERENCES

(1) Birdja, Y. Y.; Pérez-Gallent, E.; Figueiredo, M. C.; Göttle, A. J.; Calle-vallejo, F.; Koper, M. T. M. Advances and Challenges in Understanding the Electrocatalytic Conversion of Carbon Dioxide to Fuels. *Nat. Energy* **2019**, *4*, 732−745.

(2) De Luna, P.; Hahn, C.; Higgins, D.; Jaffer, S. A.; Jaramillo, T. F.; Sargent, E. H. What Would It Take for Renewably Powered Electrosynthesis to Displace Petrochemical Processes? *Science* **2019**, *364*, No. eaav3506.

(3) Shin, H.; Hansen, K. U.; Jiao, F. Techno-Economic Assessment of Low-Temperature Carbon Dioxide Electrolysis. *Nat. Sustainability* **2021**, *4*, 911−919.

(4) Raya-Imbernón, A.; Samu, A. A.; Barwe, S.; Cusati, G.; Fődi, T.; Hepp, B. M.; Janáky, C. Renewable Syngas Generation via Low-Temperature Electrolysis: Opportunities and Challenges. *ACS Energy Lett.* **2024**, *9*, 288−297.

(5) Hori, Y.; Wakebe, H.; Tsukamoto, T.; Koga, O. Electrocatalytic Process of CO Selectivity in Electrochemical Reduction of CO_2 at Metal Electrodes in Aqueous Media. *Electrochim. Acta* **1994**, *39* (11−12), 1833−1839.

(6) Bagger, A.; Ju, W.; Varela, A. S.; Strasser, P.; Rossmeisl, J. Electrochemical CO_2 Reduction: A Classification Problem. *ChemPhysChem* **2017**, *18*, 3266−3273.

(7) Mukhopadhyay, S.; Naeem, M. S.; Shiva Shanker, G.; Ghatak, A.; Kottaichamy, A. R.; Shimoni, R.; Avram, L.; Liberman, I.; Balilty, R.; Ifraemov, R.; Rozenberg, I.; Shalom, M.; López, N.; Hod, I. Local CO_2 Reservoir Layer Promotes Rapid and Selective Electrochemical CO_2 Reduction. *Nat. Commun.* **2024**, *15*, No. 3397.

(8) Rosen, B. A.; Salehi-khojin, A.; Thorson, M. R.; Zhu, W.; Whipple, D. T.; Kenis, P. J. A.; Masel, R. I. Ionic Liquid-Mediated Selective Conversion of CO_2 to CO at Low Overpotentials. *Science* **2011**, *334*, 643−644.

(9) Rosen, B. A.; Haan, J. L.; Mukherjee, P.; Braunschweig, B.; Zhu, W.; Salehi-Khojin, A.; Dlott, D. D.; Masel, R. I. In Situ Spectroscopic Examination of a Low Overpotential Pathway for Carbon Dioxide Conversion to Carbon Monoxide. *J. Phys. Chem. C* **2012**, *116*, 15307−15312.

(10) Ohlin, C. A.; Dyson, P. J.; Laurenczy, G. Carbon Monoxide Solubility in Ionic Liquids: Determination, Prediction and Relevance to Hydroformylation. *Chem. Commun.* **2004**, *4*, 1070−1071.

(11) Cadena, C.; Anthony, J. L.; Shah, J. K.; Morrow, T. I.; Brennecke, J. F.; Maginn, E. J. Why Is CO_2 so Soluble in Imidazolium-Based Ionic Liquids? *J. Am. Chem. Soc.* **2004**, *126*, 5300−5308.

(12) Bohra, D.; Chaudhry, J. H.; Burdyny, T.; Pidko, E. A.; Smith, W. A. Modeling the Electrical Double Layer to Understand the Reaction Environment in a CO_2 Electrocatalytic System. *Energy Environ. Sci.* **2019**, *12*, 3380−3389.

(13) Cargill, W. R. Solubility Data Series Volume 43 Carbon Monoxide *IUPAC Solubility Data Series* 1990; Vol. *43*.

(14) Chen, L. D.; Urushihara, M.; Chan, K.; Nørskov, J. K. Electric Field Effects in Electrochemical CO_2 Reduction. *ACS Catal.* **2016**, *6*, 7133−7139.

(15) Fortunati, A.; Risplendi, F.; Re Fiorentin, M.; Cicero, G.; Parisi, E.; Castellino, M.; Simone, E.; Iliev, B.; Schubert, T. J. S.; Russo, N.; Hernández, S. Understanding the Role of Imidazolium-Based Ionic Liquids in the Electrochemical CO_2 Reduction Reaction. *Commun. Chem.* **2023**, *6*, 84.

(16) Monteiro, M. C. O.; Dattila, F.; Hagedoorn, B.; García-Muelas, R.; López, N.; Koper, M. T. M. Absence of CO_2 Electroreduction on Copper, Gold and Silver Electrodes without Metal Cations in Solution. *Nat. Catal.* **2021**, *4*, 654−662.

(17) Urushihara, M.; Chan, K.; Shi, C.; Nørskov, J. K. Theoretical Study of $EMIM^+$ Adsorption on Silver Electrode Surfaces. *J. Phys. Chem. C* **2015**, *119*, 20023−20029.

(18) Sharifi Golru, S.; Biddinger, E. J. Effect of Anion in Diluted Imidazolium-Based Ionic Liquid/Buffer Electrolytes for CO_2 Electroreduction on Copper. *Electrochim. Acta* **2020**, *361*, No. 136787.

(19) Neyrizi, S.; Kiewiet, J.; Hempenius, M. A.; Mul, G. What It Takes for Imidazolium Cations to Promote Electrochemical Reduction of CO_2. *ACS Energy Lett.* **2022**, *7*, 3439−3446.

(20) Feaster, J. T.; Jongerius, A. L.; Liu, X.; Urushihara, M.; Nitopi, S. A.; Hahn, C.; Chan, K.; Nørskov, J. K.; Jaramillo, T. F. Understanding the Influence of [EMIM]Cl on the Suppression of the Hydrogen Evolution Reaction on Transition Metal Electrodes. *Langmuir* **2017**, *33*, 9464−9471.

(21) Wang, Y.; Hatakeyama, M.; Ogata, K.; Wakabayashi, M.; Jin, F.; Nakamura, S. Activation of CO_2 by Ionic Liquid EMIM−BF_4 in the Electrochemical System: A Theoretical Study. *Phys. Chem. Chem. Phys.* **2015**, *17*, 23521−23531.

(22) Sun, L.; Ramesha, G. K.; Kamat, P. V.; Brennecke, J. F. Switching the Reaction Course of Electrochemical CO_2 Reduction with Ionic Liquids. *Langmuir* **2014**, *30*, 6302−6308.

(23) Kemna, A.; García Rey, N.; Braunschweig, B. Mechanistic Insights on CO_2 Reduction Reactions at Platinum/[BMIM][BF_4] Interfaces from in Operando Spectroscopy. *ACS Catal.* **2019**, *9*, 6284−6292.

(24) Sharifi Golru, S.; May, A. S.; Biddinger, E. J. Modifying Copper Local Environment with Electrolyte Additives to Alter CO_2 Electroreduction vs Hydrogen Evolution. *ACS Catal.* **2023**, *13*, 7831−7843.

(25) Moya, C.; Alonso-Morales, N.; Gilarranz, M. A.; Rodriguez, J. J.; Palomar, J. Encapsulated Ionic Liquids for CO_2 Capture: Using 1-Butyl-Methylimidazolium Acetate for Quick and Reversible CO_2 Chemical Absorption. *ChemPhysChem* **2016**, *17*, 3891−3899.

(26) Mao, J. X.; Steckel, J. A.; Yan, F.; Dhumal, N.; Kim, H.; Damodaran, K. Understanding the Mechanism of CO_2 Capture by 1,3 di-Substituted Imidazolium Acetate Based Ionic Liquids. *Phys. Chem. Chem. Phys.* **2016**, *18*, 1911−1917.

(27) Yan, F.; Dhumal, N. R.; Kim, H. J. CO_2 Capture in Ionic Liquid 1-Alkyl-3-Methylimidazolium Acetate: A Concerted Mechanism without Carbene. *Phys. Chem. Chem. Phys.* **2017**, *19*, 1361−1368.

(28) Chiarotto, I.; Feroci, M.; Inesi, A. First Direct Evidence of N-Heterocyclic Carbene in BMIM Acetate Ionic Liquids. An Electrochemical and Chemical Study on the Role of Temperature. *New J. Chem.* **2017**, *41*, 7840−7843.

(29) Moya, C.; Palomar, J.; Gonzalez-Miquel, M.; Bedia, J.; Rodriguez, F. Diffusion Coefficients of CO_2 in Ionic Liquids Estimated by Gravimetry. *Ind. Eng. Chem. Res.* **2014**, *53*, 13782−13789.

(30) Perdew, J. P.; Burke, K.; Ernzerhof, M. Generalized Gradient Approximation Made Simple. *Phys. Rev. Lett.* **1996**, *77*, 3865−3868.

(31) Bard, A. J.; Faulkner, L. R. *Electrochemical Methods: Fundamentals and Application*; John Wiley & Sonds, Inc., 2001.

(32) Ohyama, J.; Okubo, K.; Ishikawa, K.; Saida, T.; Yamamoto, Y.; Arai, S.; Satsuma, A. Removal of Surface Poisoning Improves Hydrogen Oxidation Performance of Pt Catalysts under Basic Conditions. *ACS Appl. Energy Mater.* **2020**, *3*, 1854−1859.

(33) Goyal, A.; Koper, M. T. M. The Interrelated Effect of Cations and Electrolyte pH on the Hydrogen Evolution Reaction on Gold Electrodes in Alkaline Media. *Angew. Chem., Int. Ed.* **2021**, *60*, 13452−13462.

(34) Pérez-Ramírez, J.; López, N. Strategies to Break Linear Scaling Relationships. *Nat. Catal.* **2019**, *2*, 971−976.

https://doi.org/10.1021/acscatal.4c05012
ACS Catal. 2024, 14, 16166−16174

(35) Hammer, B.; Nørskov, J. K. Why Gold Is the Noblest of All the Metals. *Nature* **1995**, *376*, 238−240.
(36) Hammer, B.; Nørskov, J. K. Electronic Factors Determining the Reactivity of Metal Surfaces. *Surf. Sci.* **1995**, *343*, 211−220.
(37) Hammer, B.; Morikawa, Y.; Nørskov, J. K. CO Chemisorption at Metal Surfaces and Overlayers. *Phys. Rev. Lett.* **1996**, *76*, 2141−2144.
(38) Álvarez-Moreno, M.; De Graaf, C.; López, N.; Maseras, F.; Poblet, J. M.; Bo, C. Managing the Computational Chemistry Big Data Problem: The IoChem-BD Platform. *J. Chem. Inf. Model.* **2015**, *55*, 95−103.
(39) Dattila, F. Descriptors IL *ioChem-BD* DOI: 10.19061/iochem-bd-1-306.

https://doi.org/10.1021/acscatal.4c05012
ACS Catal. 2024, 14, 16166−16174